Configurational Electronic Entropy and the Phase Diagram of Mixed-Valence Oxides: The Case of Li_xFePO_4

Fei Zhou,[1] Thomas Maxisch,[2] and Gerbrand Ceder[2]

[1]*Department of Physics, Massachusetts Institute of Technology, Cambridge, Massachusetts 02139, USA*

[2]*Department of Materials Science and Engineering, Massachusetts Institute of Technology, Cambridge, Massachusetts 02139, USA*

(Received 19 July 2006; published 13 October 2006)

We demonstrate that configurational electronic entropy, previously neglected, in *ab initio* thermodynamics of materials can qualitatively modify the finite-temperature phase stability of mixed-valence oxides. While transformations from low-T ordered or immiscible states are almost always driven by configurational disorder (i.e., random occupation of lattice sites by multiple species), in $FePO_4$-$LiFePO_4$ the formation of a solid solution is almost entirely driven by electronic rather than ionic configurational entropy. We argue that such an electronic entropic mechanism may be relevant to most other mixed-valence systems.

DOI: 10.1103/PhysRevLett.97.155704 PACS numbers: 64.75.+g, 65.40.Gr, 71.15.Mb, 82.47.Aa

First-principles prediction of a crystalline material's phase diagram based on density functional theory (DFT) is a prime example of the achievement of modern solid state physics [1]. A pure DFT approach is applicable to zero temperature (zero T). To study the finite-T phase stability, one has to identify carefully all the excitations and degrees of freedom involved in creating entropy. Typically in alloy theory the focus is on the configurational disorder [substitution of different elements or vacancies (V)], while the electronic degrees of freedom are, in the spirit of the adiabatic approximation, integrated out [1,2] (phonon contributions may give quantitative corrections [3–5], especially in systems with exotic electron-phonon coupling [6], but they are relatively composition insensitive and will not be discussed here). For example, many phase diagrams can be satisfactorily reproduced by considering the configurational entropy of two elements [1] or element and vacancy [7]. Electronic entropy is usually thought of as a small quantitative correction and can be calculated from the band structure [8,9]:

$$S_e^{\text{band}} = -k_B \int n[f \ln f + (1-f)\ln(1-f)]dE, \qquad (1)$$

where n and f are the density of states and Fermi distribution function, respectively. Only electrons within $\sim k_B T$ to the Fermi level participate in the excitations, so S_e^{band} is usually small. A different type of electronic entropy could arise if electrons (e) or holes (h) are localized and contribute to the total entropy in the same fashion as the ordering of atoms. One would expect such configurational electronic entropy to be particularly important in mixed-valence transition metal oxides. Many technologically important materials, such as doped manganites, high-T superconductors, Na- and Li-metal oxides, and mixed conductors, fall in this category. Little is known about the contribution of localized e-h to finite-T phase stability, though previous evidence exists in doped superconductors [10,11] and perovskites [12] that a configurational electronic entropy term (assuming random e-h distribution),

$$S_e^{\text{loc,rand}} = -k_B[x \ln x + (1-x)\ln(1-x)], \qquad (2)$$

helps explain the entropy of oxidation or reduction. In Eq. (2) x is the concentration of localized electrons or holes. While $S_e^{\text{loc,rand}}$ can potentially be as significant as the configurational entropy of ions, there currently exists no clear demonstration that electronic entropy can qualitatively modify finite-T phase diagram.

In this Letter we investigate the effects of configuration-dependent electronic entropy. We go beyond a random model such as Eq. (2) and sample electron configurations explicitly. We focus on the Li_xFePO_4 system. While its high intrinsic Li^+ mobility makes it of interest as the next-generation cathode for rechargeable Li batteries [13], it also ensures good phase equilibration, even at room temperature (RT). So Li_xFePO_4 is a good system to benchmark theory against. We show that excellent agreement with the experimental phase diagram can be achieved only by taking into account configurational electronic entropy, and qualitative discrepancies occur if the electron degree of freedom is ignored.

$LiFePO_4$ has an olivine-type structure with an orthorhombic unit cell (Fig. 1). Li removal at RT occurs through a miscibility gap between triphylite (T) $LiFePO_4$ and heterosite (H) $FePO_4$ [13] with both phases having a very limited amount of solubility [vacancies + holes (Fe^{3+}) in T and Li^+ ions + electrons (Fe^{2+}) in H] [14]. Recent higher-T investigations of the Li_xFePO_4 phase diagram by Delacourt *et al.* [15] and by Dodd *et al.* [16] confirm the low-T immiscibility, but also find an unusual eutectoid point at 150 °C [15] or 200 °C [16] where the solid solution (SS) phase emerges around $x \approx 0.45$–0.65. Above 300–400 °C, SS dominates all compositions.

This phase diagram is quite unexpected from a theoretical point of view. First, why does the system phase separate

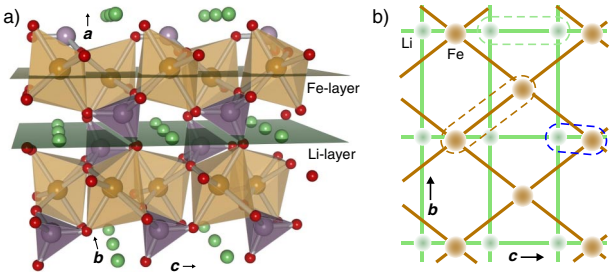

FIG. 1 (color online). The $LiFePO_4$ structure shown with (a) PO_4 (purple) and FeO_6 (brown) polyhedra as well as Li atoms (green), and (b) adjacent layers on Li and Fe sublattices, projected along axis a, with nearest-neighbor inter- and intralattice pairs highlighted.

at all at low-T? In a simplified picture of a generic oxide Li_xMO_n, the Li^+ ions repel each other due to electrostatics so that ordered intermediate compounds are energetically favorable over phase separation, i.e., segregation of Li^+ (vacancies) into Li-rich (deficient) regions. This is indeed the case in many other materials, in which mobile ions and vacancies coexist, e.g., Li_xCoO_2, Li_xNiO_2, or Na_xCoO_2 [7,17,18]. Second, what is the origin of the complex high-T behavior? Transitions from a two-phase coexistence state to a solid solution are typically driven by the configurational entropy of the ions in the SS, with a maximum transition T near equiatomic A, B composition. The experimentally established phase diagram is unlikely to come from such ionic configurational entropy unless the effective Li-V interactions are unusually strongly composition dependent. We demonstrate that the topology arises from electron degrees of freedom which stabilize the SS near $x \approx 0.5$.

We study the Li_xFePO_4 phase diagram by Monte Carlo simulations based on a coupled cluster expansion [19,20], which is a Hamiltonian that explicitly describes the dependence of the energy on the arrangement of Li^+/V and Fe^{2+}/Fe^{3+}, i.e., both ionic and electronic degrees of freedom. In Li_xFePO_4 the Li^+ ions and vacant sites sit on an orthorhombic lattice, of which one layer is shown in Fig. 1(b) (large green points). On each side of this Li layer is a plane of Fe sites (only one plane shown in small brown points). Representing with $\lambda_i = \pm 1$ occupation of site i by a Li^+ or vacancy and with $\epsilon_a = \pm 1$ the presence of Fe^{2+} (electron) or Fe^{3+} (hole) on site a, the energy can be expanded without loss of generality in polynomials of these occupation variables [19,20]:

$$E[\vec{\lambda}, \vec{\epsilon}] = J_\varnothing + J_i\lambda_i + J_{ij}\lambda_i\lambda_j + J_{ia}\lambda_i\epsilon_a + J_{ab}\epsilon_a\epsilon_b + \cdots. \quad (3)$$

The expansion coefficients J are called effective cluster interactions (ECIs), essentially coupling constants in a generalized Ising model. In its untruncated form, Eq. (3) is exact and includes all multibody terms within one sublattice (Li/V or e-h) and between sublattices, though some truncation takes place in practice. To parametrize Eq. (3) we have performed generalized gradient approximation + U (GGA + U) calculations for 245 Li_xFePO_4 ($0 \le x \le 1$) configurations with supercells of up to 32 f.u. using parameter $U - J = 4.3$ eV [21] and other settings in [21,22]. For each Li/V configuration, usually more than one e-h configuration was considered. The GGA + U [23] approach is essential to properly localize electronic states (polarons) in this material [22,24]. Removal of the self-interaction through proper treatment of the on-site electron correlation of localized d electrons in GGA + U has previously shown to accurately reproduce the band gap [25], lithium insertion voltage [21,26,27], and low-T immiscibility [22], unlike uncorrected local-density approximation (LDA) or GGA which incorrectly predict stable intermediate Li_xFePO_4 compounds [22]. Ferromagnetic high-spin Fe ions are assumed. At RT (Li)$FePO_4$ is paramagnetic [28] and energetic effects of magnetic ordering are small [22], so the spin entropy ($\approx k_B[x \ln 5 + (1 - x)\ln 6]$) is linear in x at RT and therefore negligible in phase diagram calculations.

Our cluster expansion model consists of 29 distinct ECIs: the constant and the point terms with no effect on the phase diagram; 7 small triplet terms, which mainly represent slight asymmetry between $FePO_4$ and $LiFePO_4$; and most significantly the 20 pair interactions shown in Fig. 2. Note that these are *effective* interactions including the effects of many physical factors: electrostatics, screening, relaxation, covalency, etc. The Li-Li ECI (diamonds) is largest for nearest-neighbor (NN) Li^+ ions, which repel each other strongly for electrostatic reasons. As the pairs are separated further, the repulsion is screened considerably. The small negative $J_{\text{Li-Li}}$ at large distance indicates some mediation of the effective interactions by lattice distortions. Roughly the same trend is observed for $J_{e\text{-}e}$. On the contrary, the Li-e interlattice ECIs are strong short-range attractions that generally become weaker at longer distance. The trend in the three curves is not monotonic, since the ECIs contain complex lattice factors beyond isotropic electrostatics. The low-T phase separation can be explained by considering the dominating short-range

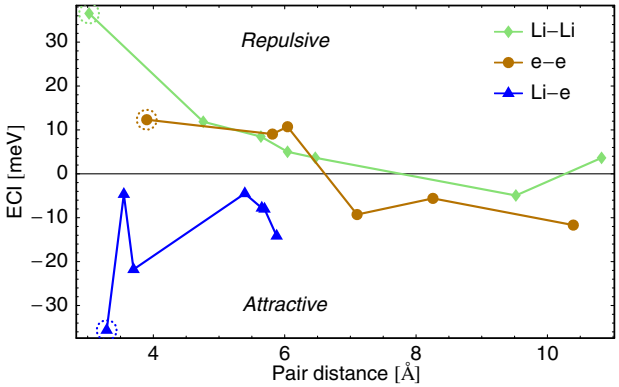

FIG. 2 (color online). Pair ECI vs site distance (measured from the sites' ideal coordinates in $LiFePO_4$). The circled points correspond to NN Li-Li, e-e, and Li-e pairs in Fig. 1(b).

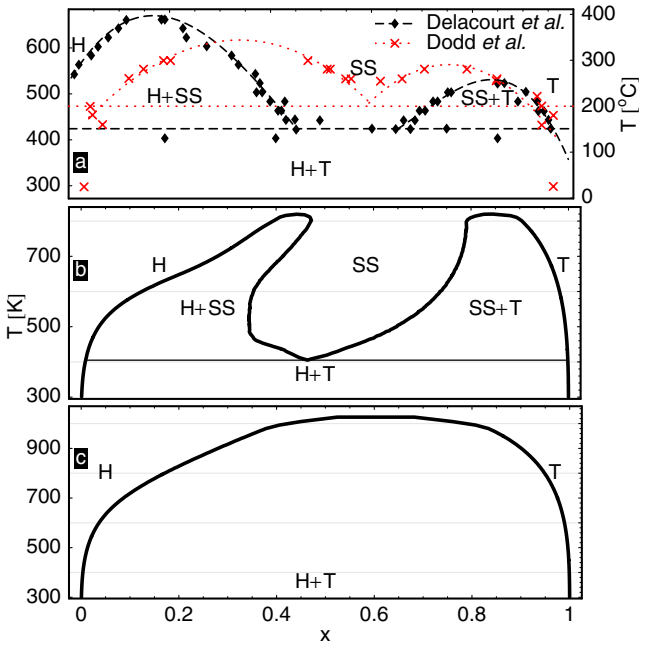

FIG. 3 (color online). Li_xFePO_4 phase diagram. (a) Experimental phase boundary data taken from Delacourt *et al.* [15] and from Dodd *et al.* [16]; (b) calculated with both Li and electron degrees of freedom and (c) with explicit Li only.

terms. The Li^+ ions repel each other and so do electrons, while Li-e attractions compete to bind them together: if Li^+ ions stay together, then the e^- can bind to more of them. The Li-e attractions prevail partly because of the host's geometry: the multiplicity of the NN Li-e ECI, the strongest attraction, is 2 per f.u., while that of NN Li-Li ECI, the strongest repulsion, is one (see Fig. 1). We therefore conclude that phase separation in Li_xFePO_4 is mainly driven by Li-e attractions in competition with Li-Li and e-e repulsions. This is fundamentally different from a system where the electronic mixed valence is delocalized, as in metallic Li_xCoO_2 [7], thereby making the Li-e coupling independent of the Li/V distribution.

Monte Carlo (MC) simulations combining canonical (interchanging Li/V or e-h pairs) and grand canonical (interchanging Li + e together into $V + h$ and vice versa) steps are carried out on a $6 \times 12 \times 12$ supercell, resulting in the phase diagram in Fig. 3(b). Phase boundaries were obtained with free energy integration. In excellent agreement with [15,16], the calculated phase diagram features a miscibility gap between $FePO_4$ and $LiFePO_4$, and an unusual eutectoid transition to the solid solution phase. The eutectoid temperature is only 20–70 K off from [15,16]. We predict the enthalpy of mixing at the eutectoid point to be 8.6 meV/f.u., consistent with the measured lower limit 700 J/mol = 7.3 meV/f.u. for an $x = 0.47$ sample [16].

To understand better which physics determines the shape of Fig. 3(b), we have also performed calculations in the more "traditional" way, i.e., to consider only the Li/V ordering as the entropy generating mechanism, assuming electrons always occupy the lowest energy state for each Li/V configuration. The calculated phase diagram [Fig. 3(c)] shows a simple two-phase region, qualitatively different from experiment but similar to typical immiscible systems. The striking difference between Figs. 3(b) and 3(c) points to the crucial importance of explicitly treating the electron degrees of freedom in excitations and finite-T thermodynamics of these mixed-valence systems.

A deeper analysis of the phase diagram in Fig. 3(b) requires investigation of the entropy driving the phase transition. The total (joint) configurational entropy $S(\mathrm{Li}, e)$ of the electronic + ionic system can be calculated through free energy integration. To partition the entropy into ionic and electronic contributions, we note that

$$S(\mathrm{Li}, e) = S'(\mathrm{Li}) + S'(e) + I(\mathrm{Li}, e), \tag{4}$$

where I is the mutual information of the 2 degrees of freedom, and $S'(X) \equiv S(X|Y) = \sum_y P(y) S(X|y)$ is the conditional entropy from the X (Li or electron) degree of freedom, i.e., the entropy contribution of X with fixed Y, thermal averaged over the marginal distribution $P(Y)$. $S'(X)$ measures how random X can be when Y is fixed. If X and Y are independent, S' is exactly the entropy contribution from 1 degree of freedom. We use S' to compare different entropy contributions. In Fig. 4 we show the total and separate entropy along the solubility limits of the H and T phases [leftmost and rightmost phase boundaries in Fig. 3(b), respectively], as well as along $x = 0.5$ in SS. At low-T the total entropy [bold lines in Fig. 4(a)] is small, slightly larger in H than in T. The solid solution phase is far from random: (1) when it first appears at the eutectoid point, its entropy is a mere $0.3k_B$; (2) the total entropy of the H phase exceeds that of SS above about 570 K even though its Li content is lower; (3) up to 900 K, well above the congruent points, the total entropy $1.1k_B$ of SS($x = 0.5$) is still smaller than (complete random) $2S_e^{\mathrm{loc,rand}}(0.5) = 1.39k_B$. The difference between $S(\mathrm{Li}, e)$

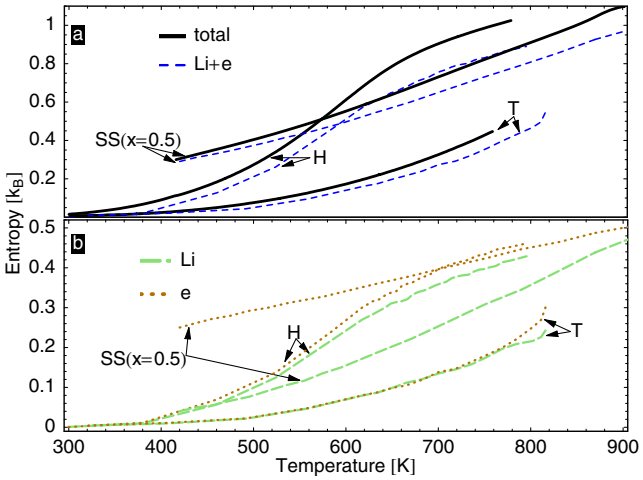

FIG. 4 (color online). Configurational entropy per formula unit: (a) total entropy and the sum $S'_{\mathrm{Li}} + S'_e$; (b) separate conditional entropy S'_{Li} and S'_e.

and $S'_{\mathrm{Li}} + S'_e$ [thin dashed curve of Fig. 4(a)] is the mutual information $I(\mathrm{Li}, e)$, indicating how correlated the 2 degrees of freedom are. Figure 4(b) shows separate S'_{Li} and S'_e in dashed and dotted curves, respectively. It is noteworthy that in all but the T branches S'_e is noticeably larger than S'_{Li}; S'_e dominates the SS phase and contributes much more than S'_{Li}. At the eutectoid point the mixing entropy driving the transition into SS is overwhelmingly electronic: $0.19k_B$ from S'_e vs $0.05k_B$ from S'_{Li}. A qualitative explanation for the larger S'_e is that the leading $J_{e\text{-}e}$ terms are weaker than the leading $J_{\mathrm{Li\text{-}Li}}$, and the electron excitation spectrum at a fixed Li configuration is lower in energy than the opposite. We therefore conclude, to the extent that S' represents a separate entropy, that the electron degree of freedom contributes substantially more than Li ions to disordering of the system, and that the formation of the solid solution state is driven by *e-h* disorder. To our knowledge, no other examples of electronic entropy-driven solid solution have been identified, though electronic entropy-driven modification of ordering interactions through band entropy has been proposed for Ni_3V [29].

Beyond $LiFePO_4$, our approach and results may help our understanding of other mixed-valence transition metal oxides with localized electrons. In oxides both electron localization and delocalization can occur. For example, a system such as Li_xCoO_2 is metallic for $x < 0.9$ [30] and explicit *e-h* entropy is less crucial. LDA and GGA in which mixed-valence states are delocalized will be an adequate treatment for such system [7]. On the other hand, materials in which carriers localize require more careful treatment both for their energy calculation (e.g., in GGA + U, SIC methods, or dynamical mean field theory [31]), and for their contribution of the electronic degree of freedom to the entropy as demonstrated in the present work. An even more complicated situation arises in materials where electrons can be exchanged between localized and delocalized states, as in Ce [32]. It should be noted that in our MC simulations, *e-h* are treated as classical particles (but not in the DFT energy calculations). If hopping becomes so fast that electron wave functions overlap, the notion of localized electrons becomes meaningless, and it becomes difficult to enumerate the eigenstates over which to sum excitations, until one reaches the nearly free-electron limit where the band picture is applicable. It is up to further investigation to establish quantitative effects of the localized electron degree of freedom in thermodynamics of other transition metal oxides.

F. Z. would like to thank A. Van der Ven for his help in computation. This work is supported by the DOE under Contract No. DE-FG02-96ER45571 and by the NSF MRSEC program under Contract No. DMR-0213282.

[1] D. de Fontaine, in *Solid State Physics*, edited by H. Ehrenreich and D. Turnbull (Academic Press, New York, 1994), Vol. 47, p. 33.
[2] G. Ceder, Comput. Mater. Sci. **1**, 144 (1993).
[3] A. van de Walle and G. Ceder, Rev. Mod. Phys. **74**, 11 (2002).
[4] M. Asta, R. McCormack, and D. de Fontaine, Phys. Rev. B **48**, 748 (1993).
[5] C. Wolverton and V. Ozolins, Phys. Rev. Lett. **86**, 5518 (2001).
[6] M. E. Manley, M. Yethiraj, H. Sinn, H. M. Volz, A. Alatas, J. C. Lashley, W. L. Hults, G. H. Lander, and J. L. Smith, Phys. Rev. Lett. **96**, 125501 (2006).
[7] A. Van der Ven, M. K. Aydinol, G. Ceder, G. Kresse, and J. Hafner, Phys. Rev. B **58**, 2975 (1998).
[8] D. M. C. Nicholson, G. M. Stocks, Y. Wang, W. A. Shelton, Z. Szotek, and W. M. Temmerman, Phys. Rev. B **50**, 14 686 (1994).
[9] C. Wolverton and A. Zunger, Phys. Rev. B **52**, 8813 (1995).
[10] P. Schleger, W. N. Hardy, and H. Casalta, Phys. Rev. B **49**, 514 (1994).
[11] R. Tetot, V. Pagot, and C. Picard, Phys. Rev. B **59**, 14 748 (1999).
[12] M. H. R. Lankhorst, H. J. M. Bouwmeester, and H. Verweij, Solid State Ionics **96**, 21 (1997).
[13] A. K. Padhi, K. S. Nanjundaswamy, and J. B. Goodenough, J. Electrochem. Soc. **144**, 1188 (1997).
[14] A. Yamada, H. Koizumi, N. Sonoyama, and R. Kanno, Electrochem. Solid State Lett. **8**, A409 (2005).
[15] C. Delacourt, P. Poizot, J. M. Tarascon, and C. Masquelier, Nat. Mater. **4**, 254 (2005).
[16] J. L. Dodd, R. Yazami, and B. Fultz, Electrochem. Solid State Lett. **9**, A151 (2006).
[17] I. Terasaki, Y. Sasago, and K. Uchinokura, Phys. Rev. B **56**, R12685 (1997).
[18] M. E. Arroyo y de Dompablo, A. Van der Ven, and G. Ceder, Phys. Rev. B **66**, 064112 (2002).
[19] J. M. Sanchez, F. Ducastelle, and D. Gratias, Physica (Amsterdam) **128A**, 334 (1984).
[20] P. D. Tepesch, G. D. Garbulsky, and G. Ceder, Phys. Rev. Lett. **74**, 2272 (1995).
[21] F. Zhou, M. Cococcioni, C. A. Marianetti, D. Morgan, and G. Ceder, Phys. Rev. B **70**, 235121 (2004).
[22] F. Zhou, C. A. Marianetti, M. Cococcioni, D. Morgan, and G. Ceder, Phys. Rev. B **69**, 201101 (2004).
[23] V. I. Anisimov, J. Zaanen, and O. K. Andersen, Phys. Rev. B **44**, 943 (1991).
[24] T. Maxisch, F. Zhou, and G. Ceder, Phys. Rev. B **73**, 104301 (2006).
[25] F. Zhou, K. S. Kang, T. Maxisch, G. Ceder, and D. Morgan, Solid State Commun. **132**, 181 (2004).
[26] F. Zhou, M. Cococcioni, K. Kang, and G. Ceder, Electrochem. Comm. **6**, 1144 (2004).
[27] O. Le Bacq and A. Pasturel, Philos. Mag. **85**, 1747 (2005).
[28] G. Rousse, J. Rodriguez-Carvajal, S. Patoux, and C. Masquelier, Chem. Mater. **15**, 4082 (2003).
[29] D. D. Johnson, A. V. Smirnov, J. B. Staunton, F. J. Pinski, and W. A. Shelton, Phys. Rev. B **62**, R11917 (2000).
[30] M. Menetrier, I. Saadoune, S. Levasseur, and C. Delmas, J. Mater. Chem. **9**, 1135 (1999).
[31] A. Georges, G. Kotliar, W. Krauth, and M. J. Rozenberg, Rev. Mod. Phys. **68**, 13 (1996).
[32] A. Svane, Phys. Rev. B **53**, 4275 (1996).